Liquation Cracking in Full-Penetration Al-Cu Welds

Keeping the weld-metal solute content above — not below — the solidification cracking range can prevent liquation cracking as well as solidification cracking

BY C. HUANG AND S. KOU

ABSTRACT. Liquation cracking in the partially melted zone (PMZ) of full-penetration aluminum welds was investigated, using the simple binary Alloy 2219 (Al-6.3Cu) to gain better understanding. The PMZ is the region outside the fusion zone where grain-boundary liquation occurs during welding. The circular-patch test was used to evaluate the crack susceptibility. Gas metal arc (GMA) welds were made with the weld metal containing 0.93, 2.32, 3.43, 6.30, and 7.55 wt-% Cu. The curves of temperature (T) vs. the solid fraction (f_S) were calculated for both the PMZ (same as the base metal) and the weld metal. The results were as follows: First, at 0.93% Cu liquation cracking was very severe; at 2.32% Cu liquation cracking decreased but solidification cracking appeared; at 3.43% Cu liquation cracking disappeared but solidification cracking was severe; and at 6.30 and 7.55% Cu neither type of cracking occurred. Second, liquation cracking either stopped or did not occur near solidification cracks. Third, the T-f_S curves did not intersect each other and they showed that, for the welds that liquation-cracked, the weld-metal f_S exceeded the PMZ f_S throughout PMZ solidification. Three things were proposed. First, liquation cracking is caused by the tensile strains induced in the solidifying PMZ by the solidifying and contracting weld metal that exceed the PMZ resistance to cracking. Under the same welding conditions, the tensile strains in the PMZ increase with increasing weld-metal f_S and workpiece restraint, and the PMZ resistance to cracking decreases with increasing liquation. Second, an aluminum weld metal higher in f_S than the PMZ throughout PMZ solidification can cause liquation cracking if the workpiece is restrained tightly, the PMZ is liquated heavily, and there is no solidification cracking in the adjacent weld metal to relax tensile strains in the PMZ. Third, raising the weld metal solute content beyond the solidification-cracking range can prevent liquation cracking as well as solidification cracking.

Introduction

The partially melted zone (PMZ) is a region immediately outside the weld metal where liquation occurs during welding because of overheating above the eutectic temperature (or the solidus temperature if the workpiece is completely solutionized before welding) (Ref. 1). This is illustrated in Fig. 1. Since the grain boundaries are liquated, intergranular cracking can occur under the tensile strains induced by welding. Significant tensile strains are induced in the workpiece when it is restrained and unable to contract (due to solidification shrinkage and thermal contraction) freely upon cooling during welding. Liquation cracking often occurs in the PMZ along the fusion boundary. Aluminum alloys are known to be susceptible to liquation cracking in the PMZ during welding. Liquation and liquation cracking in aluminum welds have been the subjects of great interest in welding (Refs. 1–20).

Metzger (Ref. 3) observed liquation cracking in full-penetration gas tungsten arc (GTA) welds of Alloy 6061 made with Al-Mg filler metals at high dilution ratios, but not in similar welds made with Al-Si filler metals at any dilution ratios. This was confirmed by subsequent studies on 6061 and similar alloys such as 6063 and 6082 (Refs. 5, 7–12).

Gittos et al. (Ref. 5) used the circular-patch test (Ref. 21) to study liquation cracking in an aluminum alloy close to Alloy 6082 in composition. Liquation cracking occurred in full-penetration GTA welds made with the Al-5Mg filler metal at high-dilution ratios (about 80%) but not with the Al-5Si filler metal at any dilution ratios. They proposed that liquation cracking occurs when the base metal solidus temperature is below the weld-metal solidus temperature.

Katoh et al. (Ref. 7), Kerr et al. (Ref. 8), and Miyazaki et al. (Ref. 9) used the Varestraint test (Refs. 22, 23) to study liquation cracking in GTA and GMA welds of 6000 alloys (partial penetration). Their results contradicted the cracking condition of Gittos et al. (Ref. 5).

Huang and Kou (Ref. 24) studied liquation cracking in partial-penetration aluminum welds of Alloy 2219. The papillary (nipple)-type penetration common in GMAW with spray transfer was found to oscillate along the weld and cause cracking. Various filler metals, including 1100, 2319, 4047, 4145, and 2319 plus extra Cu, were used but did not eliminate liquation cracking.

Cross and Gutscher (Ref. 25) studied the effect of Cu and Fe content on the solidification cracking and liquation in Alloy 2519 using a circular-patch test.

The present study demonstrates the significant effect of the weld-metal solute content on liquation cracking in full-penetration welds. Alloy 2219 is selected, not as the subject of investigation, but as a tool for better understanding of liquation cracking.

KEY WORDS

Aluminum
Alloy 2219
Solidification Cracking
Liquation Cracking
Partially Melted Zone
Circular-Patch Test
Scheil Equation

Experimental Procedure

The circular-patch test (Ref. 21) was used to evaluate the susceptibility to liquation cracking. As shown in Fig. 2, the workpiece was highly restrained (by being bolted down to a thick stainless steel plate) in order to prevent it from contracting freely during welding. This allows

C. HUANG and S. KOU are respectively Graduate Student and Professor in the Department of Materials Science and Engineering, University of Wisconsin, Madison, Wis.

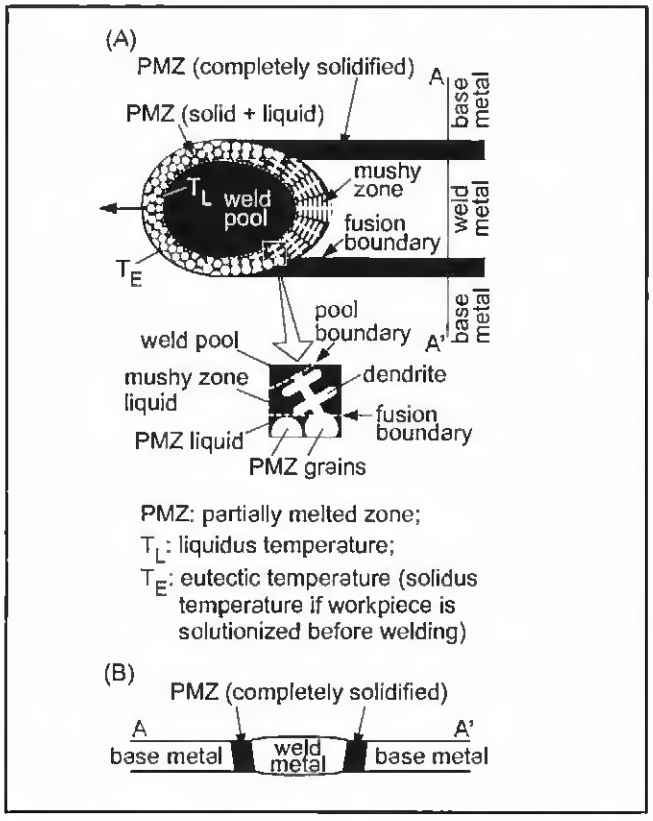

Fig. 1 — Formation of partially melted zone next to fusion boundary: A — top view; B — transverse cross section along AA' in A.

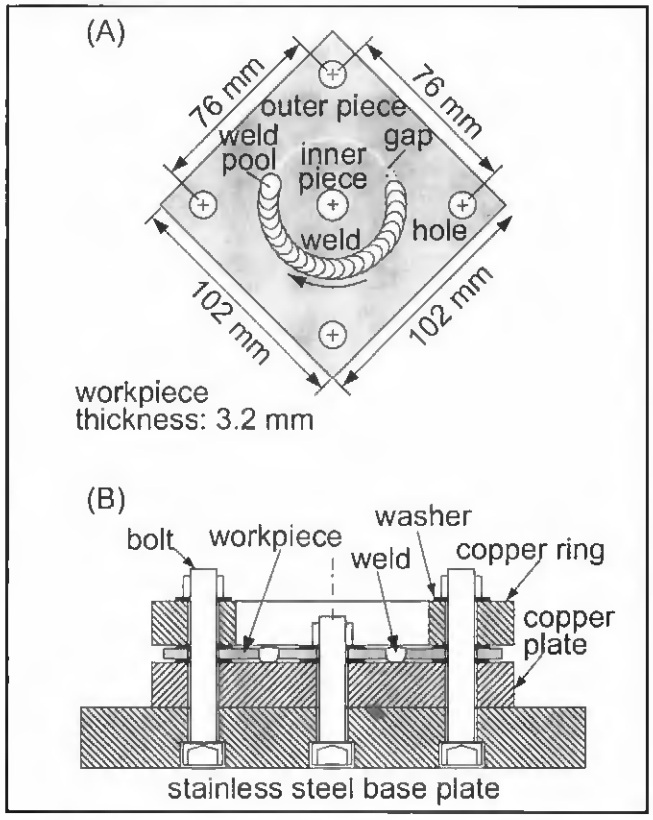

Fig. 2 — Circular-patch test. A — Top view of workpiece; B — side view of apparatus.

cracking to occur and be evaluated.

Alloy 2219-O was welded in the as-received condition, where the O-temper stands for overaging (Ref. 26). The actual compositions of the alloys and filler metals are listed in Table 1.

The workpiece consisted of two pieces. The outer piece was Alloy 2219, the inner piece was either Alloy 2219 or 1100, and filler metal was Alloy 1100, 2319, or 2319 plus extra Cu. By using different alloys as the inner piece and the filler metal, the weld-metal composition could be varied over a wide range.

The outer piece was 102 mm long, 102 mm wide and 3.2 mm thick, with a hole of 11.1 mm diameter in each corner. The inner piece was a circular patch 57.2 mm in diameter, with a hole of 12.7 mm at the center. The gap between the outer and inner pieces was about 0.25 mm. In one weld (Weld 2219/1100/1100B), the diameter of the inner piece (the circular patch) was changed to 50.8 mm to help adjust the weld-metal composition.

The outer piece was sandwiched between a copper plate (152 × 152 × 19 mm) at the bottom and a copper ring (19 mm thick, 83-mm ID, and 152 × 152 mm on the outside) at the top. The workpiece together with the copper plate and the copper ring were bolted down tightly to a stainless steel base plate of 203 × 203 × 25.4 mm. The bolts were tightened with a torque wrench to the same torque of 47.5 N·m to ensure consistent restraint conditions. A similar design was used by Nelson et al. (Ref. 27) for assessing solidification cracking in steel welds.

Table 1 — Compositions of Workpiece and Filler Metals in wt-%

	Cu	Mn	Mg	Cr	Zn	Ti	Si	Fe	Zr
					Workpiece				
1100	0.10	0.01	—	—	0.01	—	—	0.78	—
2219	6.30	0.33	—	—	0.01	0.03	0.08	0.12	0.12
					Filler Metals				
1100	0.08	0.01	—	—	0.02	—	0.08	0.52	—
2319	6.30	0.30	—	—	—	0.15	0.10	0.15	0.18

The workpiece was separated from the copper plate and the copper ring by washers (1.6 mm thick, 12.2-mm ID, and 23.5-mm OD). Without the washers, it was difficult to make full-penetration welds because of the heat sink effect of copper.

The extra Cu was a 99.999%-pure Cu wire of 1 mm diameter. When it was used, it was positioned in a 1-mm-deep groove of 50.8 mm diameter at the top surface of the circular patch. The Cu wire was placed in a 1-mm-wide groove. The extra Cu was GTA welded first to melt and mix with the surrounding base metal. The conditions for GTAW were 16 V, 75 A DCEN, and 7.4 mm/s welding speed (based on a rotation speed of 2.8 rpm and diameter of 50.8 mm) with Ar shielding. The resultant weld head was fully penetrating and about 4 mm wide at the top, well within, and thus, fully incorporated into the subsequent GMA weld.

The welding parameters for GMAW were 4.2 mm/s welding speed (based on a 1.6-rpm rotation speed and a 50.8 mm diameter), 22-V, 140-A average current, and Ar shielding. The filler wire, 1.2 mm in diameter, was positioned at 25.4 mm from the center of the workpiece, and was fed at a speed of 93.1 mm/s. The distance between the contact tube and workpiece was about 25.4 mm, and the torch was perpendicular to the workpiece.

The macrostructure and microstruc-

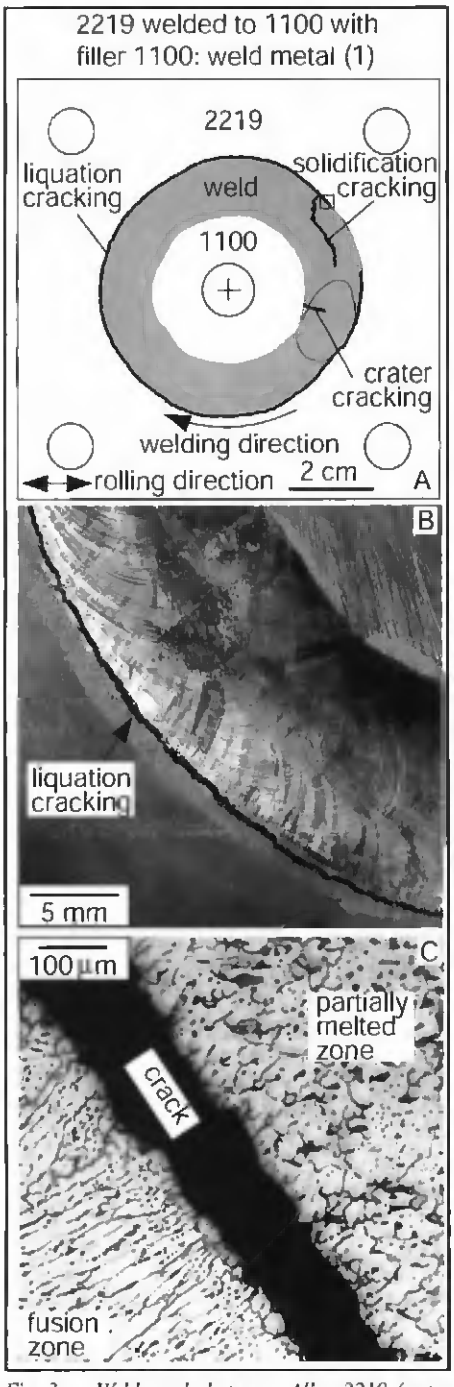

Fig. 3 — Weld made between Alloy 2219 (outer piece) and Alloy 1100 (patch of 57.2 mm diameter) with filler metal 1100. A — Overview; B — macrograph; C — micrograph of area in square in A.

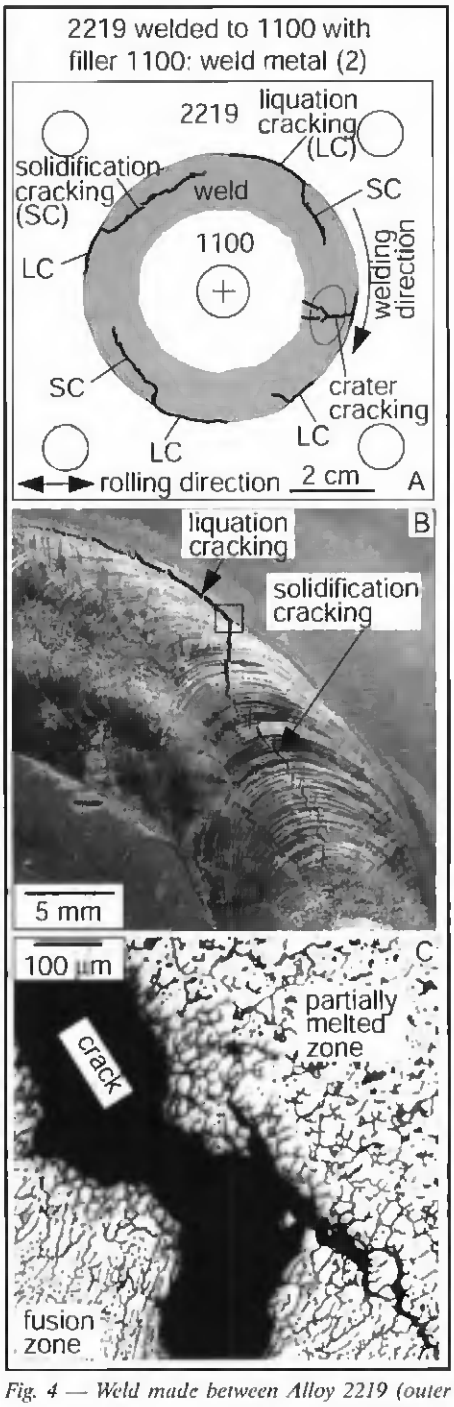

Fig. 4 — Weld made between Alloy 2219 (outer piece) and Alloy 1100 (patch of 50.8 mm diameter) with filler metal 1100. A — Overview; B — macrograph; C — micrograph of area in square in B.

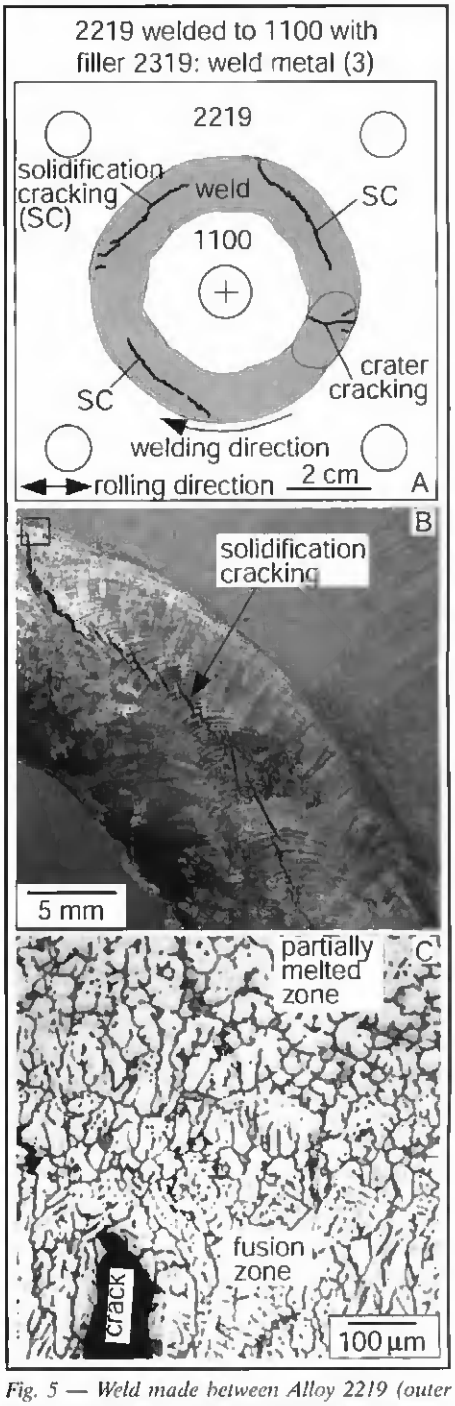

Fig. 5 — Weld made between Alloy 2219 (outer piece) and Alloy 1100 (patch of 57.2 mm diameter) with filler metal 2319. A — Overview; B — macrograph; C — micrograph of area in square in B.

ture of the resultant welds were examined. The surfaces of the resultant welds were cleaned with a solution of 48 vol-% HF in H_2O. Macrographs of the welds were taken with a digital camera. The welds were then sectioned and etched with a solution of 0.5 vol-% HF in water. The transverse cross-sectional area of each weld was determined with the help of computer software. The weld microstructure was examined with an optical microscope.

It has been shown that the composition of a single-pass GMA aluminum weld is essentially uniform (Ref. 28). The Lorenz force, surface-tension gradients, and droplet impingement help mix the filler metal with the melted base metal (Ref. 1). Thus, the concentration of an alloying element E in the weld metal was calculated from those in the base metals and the filler metal using the following equation:

$$\%\ \text{element}\ E\ \text{in weld metal} = [(\%E\ \text{in base metal}\ A) \times a + (\%E\ \text{in base metal}\ B) \times b + (\%E\ \text{in filler metal}\ C) \times c] / (a + b + c) \quad (1)$$

where the areas a, b, and c are the areas in the weld transverse cross section that represent contributions from the base metal

A, base metal *B*, and filler metal *C*, respectively. They were determined from the area and location of the transverse cross section of the weld.

Results and Discussion

The percentage contributions from the inner piece, the outer piece, and the filler metal to the welds and the resultant weld-metal compositions are listed in Table 2. The experimental results are summarized in Table 3. For convenience, all welds are identified with a series of three numbers. The first, second, and third numbers refer to the outer piece, the inner piece (circular patch), and the filler metal used, respectively. For instance, Weld 2219/1100/2319 refers to a weld made by joining an outer piece of Alloy 2219 to an inner piece of Alloy 1100 with a filler metal of Alloy 2319.

Overviews: Macrographs and Micrographs of Welds

There were two 2219/1100/1100 welds. The one with a circular patch of 57.2 mm diameter will be called Weld 2219/1100/1100A, and the one (and the only one in the present study) with a circular patch of 50.8 mm diameter, called 2219/1100/1100B.

Figure 3A is the overview of the top of Weld 2219/1100/1100A that has been traced with the help of computer software from the digital photograph of the weld. The cracks were marked with thick lines for clarity. Such an overview was used instead of the photograph itself because cracks were too small to see at the magnification of the overview. The crater at the termination of welding was included in the figure but not the beginning of the weld (at the three o'clock position of the weld), which was welded over and replaced by the crater.

Weld 2219/1100/1100A had a weld-metal composition of Al-0.93Cu. As shown in Fig. 3A, it suffered from very severe liquation cracking (91% of the weld outer edge) and some solidification cracking (13% of the weld length). Figure 3B is a macrograph of the lower left region of the weld. Liquation cracking was evident along the outer edge of the weld, but there was no liquation cracking along the inner edge. In circular-patch welding, the workpiece is held tightly against a strong back (the stainless steel base plate in Fig. 2). This keeps the weld metal from contracting due to thermal contraction and solidification shrinkage when it cools. Consequently, the outer edge of the weld is in tension while the inner edge is in compression. This explains why liquation cracking was observed only along the outer edge of the weld.

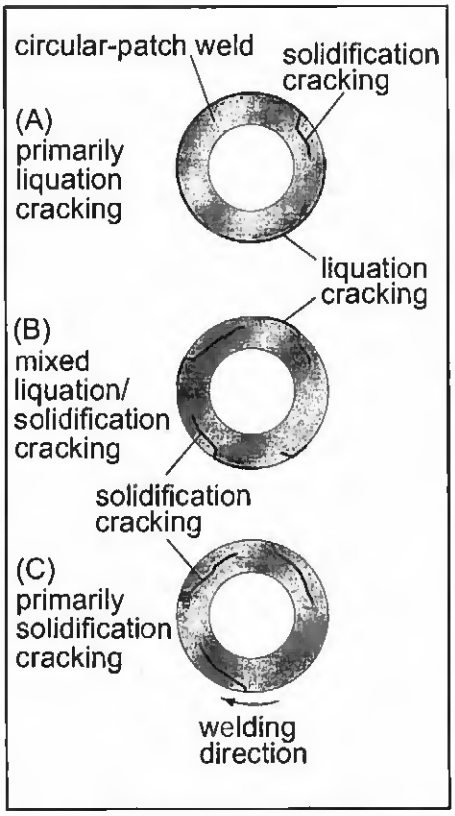

Fig. 6 — Three types of cracking observed. A — Primarily liquation cracking; B — mixed liquation/solidification cracking; C — primarily solidification cracking.

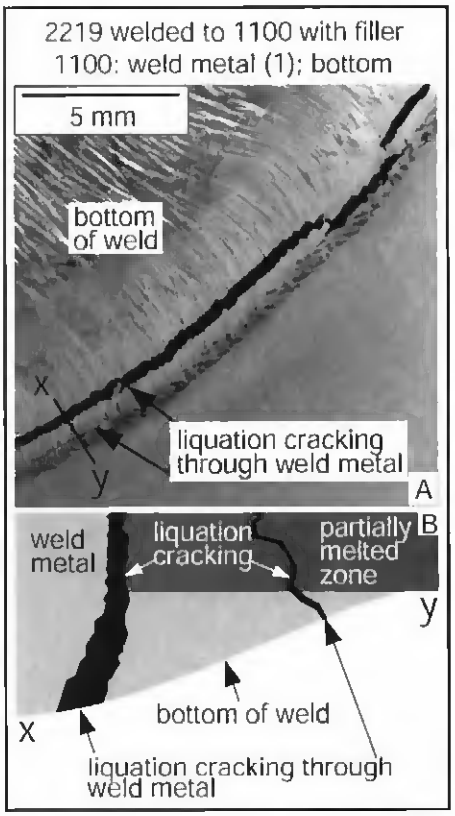

Fig. 7 — Cracking at bottom of weld. A — Bottom surface of weld in Fig. 3B; B — transverse cross section along line "xy," sketched according to micrograph observed (not shown due to space limit).

Figure 3C shows the microstructure inside the small square in Fig. 3A. The cellular/dendritic fusion zone was clearly different from the liquated PMZ. The liquation crack made a clear-cut separation of the two zones along the fusion boundary. No liquation cracking was observed inside the PMZ.

The weld-metal composition was raised to Al-2.32Cu in Weld 2219/1100/1100B to reduce liquation cracking. As shown in Fig. 4A, solidification cracking (49% of the weld length) was more and liquation cracking (28% of the outer weld edge) was less than those in Weld 2219/1100/1100A. Mixed liquation/solidification cracking was observed in four regions along the outer edge of the weld. It is interesting to note that in each region liquation cracking and solidification cracking did not coexist, that is, run side by side. Figure 4B shows cracking in the upper right region of the weld. It is evident that liquation cracking stopped at the point where solidification cracking started. This is probably because solidification cracking in the weld metal reduced the tensile strains in the adjacent PMZ significantly. In fact, a similar trend also was seen in the upper right region of Weld 2219/1100/1100A — Fig. 3A.

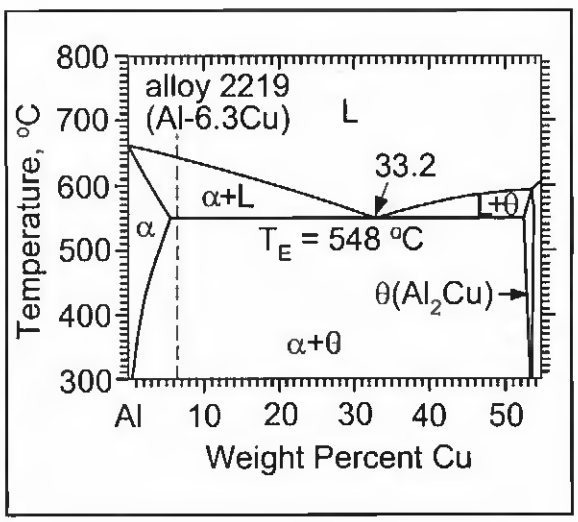

Fig. 8 — Aluminum-rich side of Al-Cu phase diagram (Ref. 30).

Table 2 — Compositions of Weld Metals

	Contribution from Outer Piece	Contribution from Inner Piece	Contribution from Filler Metal	Contribution from Extra Cu	Weld-Metal Composition
Weld metal (1) of weld 2219/1100/1100A	13.5% from 2219	52.3% from 1100	34.2% from 1100	—	Al-0.93Cu
Weld metal (2) of weld 2219/1100/1100B	36.0% from 2219	28.8% from 1100	35.2% from 1100	—	Al-2.32Cu
Weld metal (3) of weld 2219/1100/2319	21.5% from 2219	46.3% from 1100	32.2% from 2319	—	Al-3.43Cu
Weld metal (4) of weld 2219/2219/2319	65.3% from 2219 (both inner and outer pieces)		34.7% from 2319	—	Al-6.30Cu
Weld metal (5) of weld 2219/2219/2319+Cu	63.14% from 2219 (both inner and outer pieces)		35.52% from 2319	1.34% from Cu	Al-7.55Cu

Table 3 — Summary of Experimental Results

	Outer Piece/Inner Piece/Filler Metal				
	Weld 2219/1100/1100A	Weld 2219/1100/1100B	Weld 2219/1100/2319	Weld 2219/2219/2319	Weld 2219/2219/2319+Cu
Weld-metal composition	Al-0.93Cu	Al-2.32Cu	Al-3.43Cu	Al-6.3Cu	Al-7.55Cu
Liquation cracking (cm)	18.42	5.82	No	No	No
Liquation cracking (% of weld outer edge)	91	28	0	0	0
Solidification cracking (cm)	2.08	8.26	9.80	No	No
Solidification cracking (% of weld length[a])	13	49	60	0	0

(a) Weld length = (length of weld outer edge plus length of weld inner edge)/2.

Figure 4C shows the microstructure in the square of Fig. 4B. The solidification crack in the fusion zone was connected to the liquation crack at the weld interface. This suggests that liquation cracking can trigger solidification cracking. However, solidification cracking can also initiate within the fusion zone by itself and does not have to initiate at liquation cracks.

The weld-metal composition was further raised to Al-3.43Cu in Weld 2219/1100/2319 to reduce liquation cracking. Solidification cracking (60% of the weld length) took over completely, that is, liquation cracking disappeared. As shown in the overview in Fig. 5A, solidification cracking occurred in three different regions of the weld, each crack being about 3 to 4 cm long.

The macrograph in Fig. 5B shows solidification cracking in the upper right region of the weld. Cracking started from near the outer edge of the weld, propagated inward, and then followed the welding direction.

Figure 5C shows the microstructure of the weld inside the square in Fig. 5B, including the tip of the solidification crack near the fusion boundary. Clearly, solidification cracking initiated within the weld metal near the outer edge of the weld, and there was no liquation cracking in the PMZ.

As the weld-metal composition was increased to Al-6.30Cu in Weld 2219/2219/2319, which is the same as the composition of Alloy 2219 (Al-6.30Cu), neither liquation cracking nor solidification cracking occurred except for some solidification cracking inside the crater.

Finally, as the weld-metal composition was increased to Al-7.55Cu in Weld 2219/2219/2319+Cu, neither liquation cracking nor solidification cracking occurred, not even in the crater. Figure 6 summarizes the three types of cracking in the welds discussed above. It includes primarily liquation cracking (Fig. 3A), mixed liquation/solidification cracking (Fig. 4A), and primarily solidification cracking — Fig. 5A.

Locations of Cracking

The tensile strains in the weld are expected to be highest in the regions between the center of the workpiece and its four corners because the workpiece was bolted down at the center and near its four corners — Fig. 2. The weld could not have been subjected to uniform constraint during welding even if the washers were removed.

When liquation cracking was severe, it occurred essentially along the entire weld, as in the case of Weld 2219/1100/1100A (91% of the outer weld edge, Fig. 3A). However, when liquation cracking was less severe, it appeared to be located more or less in three regions: between the center of the workpiece and its lower left, upper left, and upper right corners. Weld 2219/1100/1100B is an example — Fig. 4A. The region between the center and the lower right corner was more complicated because of the overlapping between the beginning and the end of the weld. The rolling direction did not appear to have a significant effect on liquation cracking.

In fact, solidification cracking also appeared to be located more or less in the same three regions. Welds 2219/1100/1100A (Fig. 3A), 2219/1100/1100B (Fig. 4A), and 2219/1100/2319 (Fig. 5A) are examples. Solidification cracking can be initiated in a weld metal with a composition highly susceptible to solidification cracking when the weld pool enters the three regions. As already mentioned, when solidification cracks open up in the weld metal, tensile strains in the adjacent PMZ are greatly reduced and liquation cracking stops (or tends not to occur). This explains why liquation cracking switched to solidification cracking in Welds 2219/1100/1100A (Fig. 3A) and 2219/1100/1100B — Fig. 4A.

Bottom View of Liquation Cracking

Figure 7A shows the bottom surface of Weld 2219/1100/1100A. The crack did not look like liquation cracking because it ran parallel to but not exactly along the outer edge of the weld. It did not look like solidification cracking, either, because it did not move toward and propagate along the weld centerline. In fact, this crack was the bottom of the liquation crack shown in Fig. 3B.

The transverse cross section along line "xy" is shown schematically in Fig. 7B. During welding the molten metal at the bottom of the weld pool spread over the bottom surface of the PMZ, that is, the bottoms of the weld metal and the PMZ overlapped. The liquation crack along the

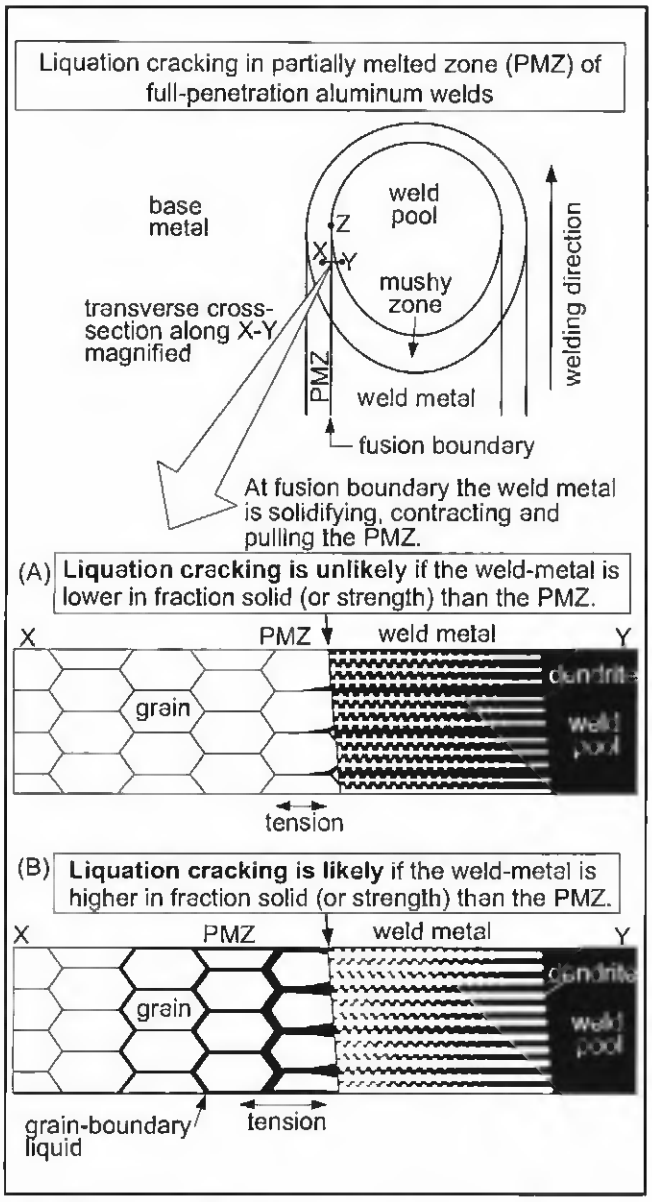

Fig. 9 — Liquation cracking in full-penetration aluminum welds: A — Liquation cracking unlikely; B — liquation cracking likely.

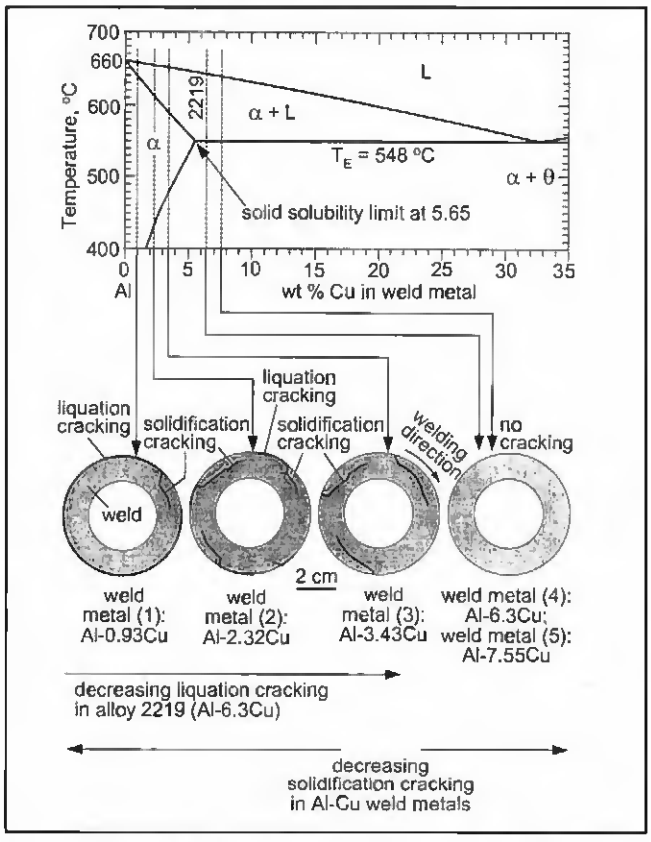

Fig. 10 — Effect of weld-metal composition on cracking in welds made in Alloy 2219.

fusion boundary propagated through the weld metal and ended up as a major crack at the bottom weld surface, while that in the PMZ also propagated through the weld metal and ended up as a minor crack at the bottom weld surface.

Mechanism of Liquation Cracking

Huang and Kou (Refs. 17, 19, 20) studied the mechanism of liquation in Alloy 2219. Figure 8 shows the Al-rich side of the Al-Cu phase diagram (Ref. 30). Cu-rich θ particles are present both along grain boundaries and within the grain interior. Upon reaching the eutectic temperature, the θ particles react with the surrounding α phase to form a eutectic liquid. Above the eutectic temperature, the eutectic liquid dissolves the surrounding α phase, increases in volume, and becomes hypoeutectic. Upon cooling, the hypoeutectic liquid solidifies first as a Cu-depleted α phase and finally as a Cu-rich eutectic.

The mechanism of liquation cracking is as follows. Liquation cracking is caused by the tensile strains induced in the solidifying PMZ by the solidifying and contracting weld metal that exceed the PMZ resistance to cracking. Therefore, liquation cracking requires the presence of both significant tensile strains in the PMZ and a susceptible PMZ microstructure.

Significant tensile strains are induced in the PMZ if the adjacent weld metal becomes stronger than the PMZ during PMZ solidification, and if the workpiece is severely restrained (for instance, in circular-patch testing) and thus unable to contract freely upon cooling. As the weld metal solidifies, it contracts because of solidification shrinkage and thermal contraction. The solidification shrinkage of aluminum is as high as 6.6% (Ref. 29). The thermal expansion coefficient of aluminum is roughly twice that of iron-based alloys. The grain-boundary liquid in the PMZ, however, does not contract significantly as it solidifies because of its much smaller volume than the weld pool. Consequently, the solidifying and contracting weld metal pulls the adjacent PMZ. The higher the solid fraction of the weld metal, the greater its strength and contraction are. For a given material, the tensile strains induced in the PMZ depend on the welding conditions, such as the heat input, welding speed, workpiece thickness, fixturing, type of weld (circular or linear), and so on. If the weld metal cracks, the tensile strains in the adjacent PMZ are relaxed. Tensile strains can also be imposed on the PMZ if external forces are applied to the workpiece during welding (for instance, in Varestraint testing).

A susceptible microstructure is present if the PMZ resistance to cracking is lowered by severe liquation. For a given material, the extent of liquation depends on the welding condition, such as the welding process, heat input, and welding speed. Therefore, for the same material under the same welding condition, the strength of the weld metal relative to that of the adjacent PMZ can have a significant effect on liquation cracking.

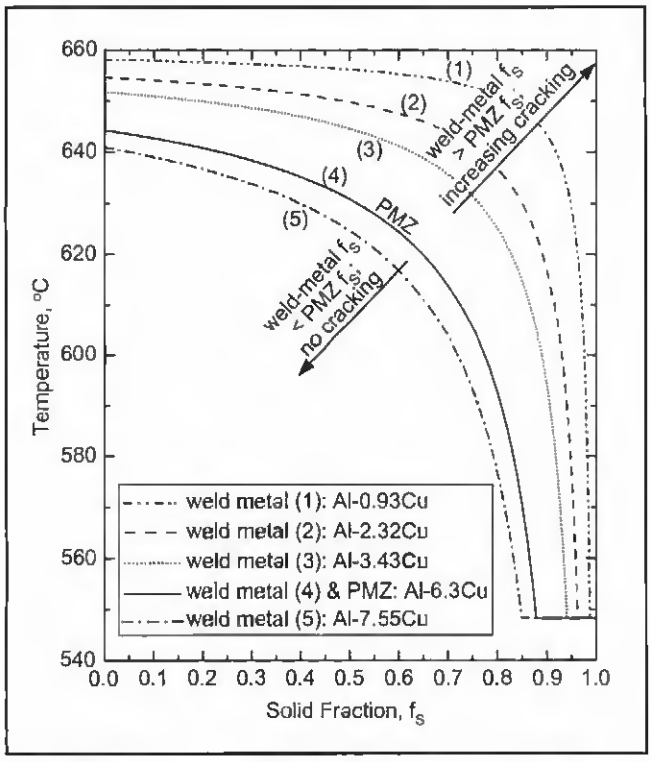

Fig. 11 — Temperature vs. solid fraction for the partially melted zone (PMZ) in Alloy 2219 and weld metals of various Cu contents.

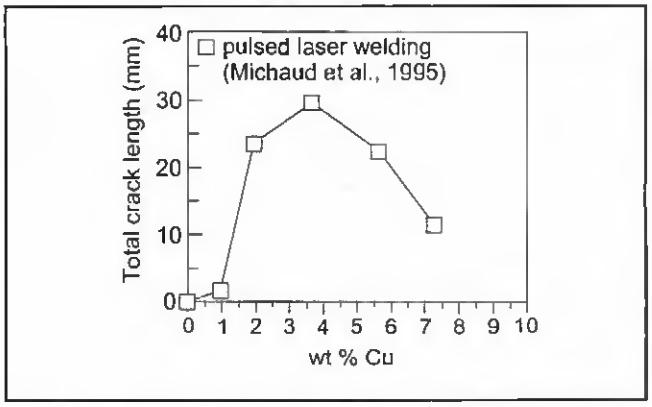

Fig. 12 — Effect of composition on solidification cracking sensitivity in pulsed laser Al-Cu welds (Ref. 33).

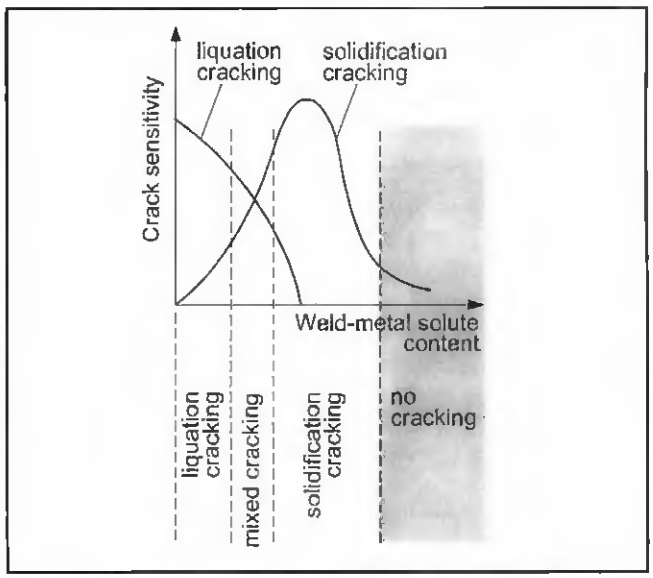

Fig. 13 — Effect of weld-metal solute content on liquation cracking and solidification cracking in full-penetration welds of a binary aluminum alloy such as 2219 (Al-6.3Cu).

Condition for Liquation Cracking

Gittos et al. (Ref. 5) proposed that liquation cracking occurs when the base-metal solidus temperature is below the weld-metal solidus temperature. However, the cooling rate during welding is too high for equilibrium solidification to exist, and solidification can continue far below the solidus temperature in an equilibrium phase diagram. A new condition for liquation cracking in full-penetration aluminum welds is proposed here.

Figure 9 shows schematically the microstructure at the fusion boundary. Consider the material at the junction between the weld pool and the fusion boundary, such as point Z. Here, the metal is completely melted both on the side of the weld pool and the side of the PMZ. As the weld pool travels a little further, the material at this point falls behind and is now at the position marked by the line XY. By now, the material has been cooling and solidifying. It consists of dendrites and interdendritic liquid on the weld-metal side, and grains and grain-boundary liquid on the PMZ side.

It is proposed that a weld metal higher in solid fraction and hence strength than the PMZ throughout PMZ solidification can cause liquation cracking if: 1) the workpiece is restrained tightly; 2) the PMZ is liquated heavily; and 3) there is no solidification cracking in the adjacent weld metal to relax the tensile strains in the PMZ. The strength of a semisolid depends primarily on the fraction of the solid phase in it, though the microstructure and the grain size can also affect the strength. Experimental data have shown that the strength of a semisolid aluminum alloy increases with increasing solid fraction (decreasing temperature) (Ref. 31).

This condition for liquation cracking in full-penetration aluminum welds is illustrated in Fig. 9. The PMZ is in tension because of the solidifying and contracting weld metal. In the case shown in Fig. 9A, at the fusion boundary the weld metal has a lower solid fraction and hence strength than the PMZ, which is only slightly liquated. Consequently, no liquation cracking occurs. In the case shown in Fig. 9B, on the other hand, at the fusion boundary the weld metal has a higher solid fraction and hence strength than the PMZ, which is severely liquated. Consequently, liquation cracking is likely to occur.

Effect of Weld-Metal Composition

Figure 10 summarizes the effect of the weld-metal composition on liquation cracking in full-penetration welds in Alloy 2219. The closer the weld-metal composition is to pure Al, the more severe liquation cracking can be. As the weld-metal Cu content increases, liquation cracking decreases.

The effect of the weld-metal composition on liquation cracking shown in Fig. 10 will be explained in the next section based on the curves of temperature vs. the solid fraction.

Temperature vs. Solid Fraction

As mentioned previously, equilibrium solidification does not exist during welding and nonequilibrium solidification needs to be considered. The simplest case of nonequilibrium solidification is that represented by the Scheil equation (Ref. 1). If the solidus line and the liquidus line

of the binary phase diagram are assumed to be straight lines, the solid fraction f_S at any given temperature T can be calculated from the following Scheil equation:

$$f_s = 1 - \left(\frac{C_o}{C_L}\right)^{\frac{1}{1-k}} \quad (2)$$

where C_o is the solute content of the alloy, C_L the composition of the liquid at the solid/liquid interface at T, and k the equilibrium partition ratio. It can be shown (Ref. 32) that the Scheil equation can be rewritten as

$$f_s = 1 - \left(\frac{(-m_L)C_o}{T_m - T}\right)^{\frac{1}{1-k}} \quad (3)$$

where m_L (< 0) is the slope of the liquidus line in the phase diagram, and T_m the melting point of pure aluminum.

Consider first the effect of the weld-metal composition on liquation cracking in Alloy 2219 — Fig. 10. According to Equation 3, at any temperature T the lower the weld-metal solute content C_o, the greater the solid fraction f_S is. That is, the stronger the solidifying weld metal becomes and causes liquation cracking. This is consistent with the effect of the Cu content shown in Fig. 10. That is, the closer the weld-metal composition is to pure Al, the higher the susceptibility of Alloy 2219 to liquation cracking is, and the susceptibility decreases as the weld-metal Cu content increases.

Figure 11 shows the T-f_S curves calculated, based on the Scheil equation, for the PMZ in Alloy 2219 and weld metals of various Cu contents. As shown, Curve 1 for the Al-0.93Cu weld metal is well on the higher-f_S side of Curve 4 for the PMZ (Al-6.3Cu). This suggests that the weld metal was higher in solid fraction and hence strength than the PMZ during solidification. This helps explain why severe liquation cracking occurred in Weld 2219/1100/1100A (Weld metal 1 in Fig. 10). Similarly, Curve 2 for the Al-2.32Cu weld metal was on the higher-f_S side of Curve 4 for the PMZ, and this explains the liquation cracking in Weld 2219/1100/1100B (Weld metal 2 in Fig. 10).

Curve 3 for the Al-3.43 Cu weld metal was also on the higher-f_S side of Curve 4 for the PMZ. Surprisingly, liquation cracking did not occur (Weld metal 3 in Fig. 10). This is probably because solidification cracking occurred first, and the tensile strains in the adjacent PMZ were thus reduced significantly before liquation cracking had a chance to occur. As will be shown later, Al-Cu alloys are most susceptible to solidification cracking between 3 and 4% Cu. Since the weld metal was highly susceptible to solidification cracking and since it reached high solid fractions before the PMZ, solidification cracking occurred before liquation cracking.

The T-f_S curve for the Al-6.3Cu weld metal coincides with Curve 4 for the PMZ. Curve 5 for the Al-7.55Cu weld metal is on the lower-f_S side of Curve 4 for the PMZ. In neither case, the solidifying weld metal has a higher solid fraction and hence strength than the PMZ to cause liquation cracking. This helps explain why liquation cracking occurred neither in Weld 2219/2219/2319 (Weld metal 4 in Fig. 10) nor Weld 2219/2219/2319+Cu (Weld metal 5 in Fig. 10).

Solidification Cracking and Liquation Cracking

Figure 12 shows the curve of solidification cracking vs. composition from Michaud et al. (Ref. 33) for the pulsed laser beam welding of binary Al-Cu alloys. As shown, the maximum crack susceptibility occurs between 3 and 4% Cu, which is close to the maximum crack susceptibility at 3.43% Cu in the present study. As shown in Fig. 10, reducing liquation cracking by increasing the Cu content can encourage solidification cracking. In view of this, the weld-metal Cu content should be increased to beyond 3 to 4% Cu in order to avoid both solidification cracking and liquation cracking. This is further illustrated in Fig. 13 (shaded area).

Comparison with Partial-Penetration Welds

As already demonstrated, in full-penetration aluminum welds, liquation cracking can be eliminated by using filler metals to adjust the weld-metal composition. As shown by Huang and Kou (Ref. 24), however, in partial-penetration welds made in Alloy 2219, liquation cracking caused by oscillation of weld penetration can persist regardless of the filler metal used because penetration oscillation allows the weld metal to solidify and hence develop strength well ahead of the PMZ regardless of the weld-metal composition. Before a new penetration front arrives and liquates the PMZ grain boundaries immediately behind it, much weld metal has already been solidifying near these grain boundaries after the previous penetration front stopped.

Summary and Conclusions

In summary, in view of the susceptibility of many aluminum alloys to liquation cracking during welding, the present study was conducted to investigate liquation cracking in full-penetration aluminum welds. The simple binary Al-Cu Alloy 2219, which is easier to understand, was selected for studying liquation cracking. To test the susceptibility to liquation cracking, circular-patch welds were made by GMAW. To vary the weld-metal composition over a wide range, Alloy 2219 was welded either to Alloy 1100 or to itself with filler metals 1100, 2319, or 2319 with extra Cu. The compositions of the resultant welds varied from 0.93 to 7.55% Cu. The macrostructure and microstructure of the welds were examined. The curves of temperature (T) vs. solid fraction (f_S), were calculated for both the weld metal and the PMZ to analyze the competition between the solidifying weld metal and the solidifying PMZ.

The conclusions are as follows:

1) *Effect of weld-metal composition.* Liquation cracking can be severe when the weld-metal solute content is low and much lower than the base-metal solute content but decreases as the weld-metal solute content increases.

2) *Effect of solidification cracking.* Solidification cracking can occur if the weld-metal composition is in the range most susceptible to solidification cracking. Liquation cracking tends to be absent near solidification cracks probably because solidification cracking relaxes the tensile strains in the nearby PMZ.

3) *T-f_S curves.* The curves for the PMZ (same as the base metal) and the weld metal, which can be calculated based on the Scheil equation, do not intersect each other in binary-alloy welds such as Al-Cu welds. They show that for the Al-Cu welds that liquation-cracked, the weld-metal f_S exceeded the PMZ f_S throughout PMZ solidification. The curves, especially when coupled with the data of solidification cracking vs. composition, help understand how liquation cracking in full-penetration aluminum welds can be avoided by adjusting the weld-metal solute content.

4) *Mechanism of liquation cracking.* Liquation cracking is caused by the tensile strains, induced in the solidifying PMZ by the solidifying and contracting weld metal, that exceed the PMZ resistance to cracking. Under the same welding conditions, the tensile strains increase with increasing weld-metal f_S and workpiece restraint, and the PMZ resistance to cracking decreases with increasing PMZ liquation.

5) *Condition for liquation cracking.* A weld metal higher in f_S than the PMZ throughout PMZ solidification can cause liquation cracking in full-penetration aluminum welds if 1) the workpiece is restrained tightly; 2) the PMZ is liquated heavily; and 3) there is no solidification cracking in the adjacent weld metal to relax the tensile strains in the PMZ. This condition is different from that of Gittos and Scott (Ref. 5) based on equilibrium solidus temperatures, that is, liquation

cracking occurs when the base-metal solidus temperature is below the weld-metal solidus temperature. Equilibrium solidification does not exist in welding.

6) *Avoiding cracking.* In the case of binary-alloy welds such as Al-Cu welds, increasing the weld-metal solute content to reduce liquation cracking can encourage solidification cracking. Decreasing the weld-metal solute content to reduce solidification cracking can encourage liquation cracking. The weld-metal composition should be adjusted to where both types of cracking can be avoided, that is, beyond the solidification cracking range.

7) *Pattern of liquation cracking.* Liquation cracking initiates at, or in the PMZ near, the outer edge of the weld and propagates along the outer edge.

8) *Pattern of solidification cracking.* Solidification cracking initiates in the weld metal near the outer edge of the weld or from liquation cracks at the outer edge and moves inward to propagate more or less along the weld centerline.

9) *Liquation cracking at weld bottom.* At the bottom surface liquation cracking may not appear at the outer edge of the weld as expected but just inside the weld metal. This can occur if the weld metal spreads slightly over the bottom surface of the PMZ, thus allowing liquation cracking to propagate through the weld metal and reach its bottom surface.

10) *Comparison with partial-penetration welds.* As demonstrated in the present study, in full-penetration aluminum welds, liquation cracking can be eliminated by using filler metals to adjust the weld-metal composition. In partial-penetration aluminum welds, however, liquation cracking near the weld root caused by oscillation of weld penetration can persist regardless of the filler metal used because penetration oscillation allows the weld metal to solidify and hence develop strength well ahead of the PMZ regardless of the weld-metal composition (Ref. 24).

Acknowledgments

This work was supported by National Science Foundation under Grant No. DMR-0098776. The authors are grateful to Bruce Albrecht and Todd Holverson of Miller Electric Manufacturing Co., Appleton, Wis., for donating the welding equipment (including Invision 456P power source, and XR-M wire feeder and gun).

References

1. Kou, S. 1987. *Welding Metallurgy*, New York, N.Y.: John Wiley and Sons, pp. 239–262, pp. 137–138, and pp. 91–108.

2. Dudas, J. H., and Collins, F. R. 1966. Preventing weld cracks in high-strength aluminum alloys. *Welding Journal* 45(6): 241-s to 249-s.

3. Metzger, G. E. 1967. Some mechanical properties of welds in 6061 aluminum alloy sheet. *Welding Journal* 46(10): 457-s to 469-s.

4. Steenbergen, J. E., and Thornton, H. R. 1970. Quantitative determination of the conditions for hot cracking during welding for aluminum alloys. *Welding Journal* 49(2): 61-s to 68-s.

5. Gittos, N. F., and Scott, M. H. 1981. Heat-affected zone cracking of Al-Mg-Si alloys. *Welding Journal* 60(6): 95-s to 103-s.

6. Ma, T., and Den Ouden, G. 1999. Liquation cracking susceptibility of Al-Zn-Mg alloys. *International Journal for the Joining of Materials* (Denmark) 11(3): 61–67.

7. Katoh, M., and Kerr, H. W. 1987. Investigation of heat-affected zone cracking of GTA welds of Al-Mg-Si alloys using the Varestraint test. *Welding Journal* 66(12): 360-s to 368-s.

8. Kerr, H. W., and Katoh, M. 1987. Investigation of heat-affected zone cracking of GMA welds of Al-Mg-Si alloys using the Varestraint test. *Welding Journal* 66(9): 251-s to 259-s.

9. Miyazaki, M., Nishio, K., Katoh, M., Mukae, S., and Kerr, H. W. 1990. Quantitative investigation of heat-affected zone cracking in aluminum Alloy 6061. *Welding Journal* 69(9): 362-s to 371-s.

10. Gittler, R., Maier, J., Muller, W., and Schwellinger, P. 1992. Formation and effect of grain boundary openings in AlMgSi alloys caused by welding. *Proceedings of 5th International Conference on Aluminum Weldments.* Ed. D. Kosteas, R. Ondra, and F. Ostermann, Munchen, Germany: Technische Universita Munchen, p. 4.1.1.

11. Powell, G. L. F., Baughn, K., Ahmed, N., Dalton, J. W., and Robinson, P. 1995. The cracking of 6000 series aluminum alloys during welding. *Proceedings of International Conference on Materials in Welding and Joining.* Parkville, Victoria, Australia: Institute of Metals and Materials Australasia.

12. Ellis, M. B. D., Gittos, M. F., and Hadley, I. 1997. Significance of liquation cracks in thick section Al-Mg-Si alloy plate. *The Welding Institute Journal* (U.K.) 6(2): 213–255.

13. Schillinger, D. E., Betz, I. G., Hussey, F. W., and Markus, H. 1963. Improving weld strength in 2000 series aluminum alloys. *Welding Journal* 42: 269-s to 275-s.

14. Young, J. G. 1968. BWRA experience in the welding of aluminum-zinc-magnesium alloys. *Welding Journal* 47(10): 451-s to 461-s.

15. Lippold, J. C., Nippes, E. F., and Savage, W. F. 1977. An investigation of hot cracking in 5083-O aluminum alloy weldments. *Welding Journal* 56(6): 171-s to 178-s.

16. Huang, C., Kou, S., and Purins, J. R. 2001. Liquation, solidification, segregation and hot cracking in the partially melted zone of Al-4.5Cu welds. *Proceedings of Merton C. Flemings Symposium on Solidification Processing.* p. 229. Ed. R. Abbaschian, H. Brody, and A. Mortensen, Warrendale, Pa.: The Mineral, Metals and Materials Society.

17. Huang, C., and Kou, S. 2000. Partially melted zone in aluminum welds — liquation mechanism and directional solidification. *Welding Journal* 79(5): 113-s to 120-s.

18. Huang, C., and Kou, S. 2002. Liquation mechanism in multicomponent aluminum alloys during welding. *Welding Journal* 81(10): 211-s to 222-s.

19. Huang, C., and Kou, S. 2001. Partially melted zone in aluminum welds — planar and celluar solidification. *Welding Journal* 80(2): 46-s to 53-s.

20. Huang, C., and Kou, S. 2001. Partially melted zone in aluminum welds — solute segregation and mechanical behavior. *Welding Journal* 80(1): 9-s to 17-s.

21. Borland, J. C., and Rogerson, J. H. 1963. Examination of the patch test for assessing hot cracking tendencies of weld metal. *British Welding Journal* 8: 494–499.

22. Savage, W. F., and Lundin, C. D. 1965. The Varestraint test. *Welding Journal* 44(10): 433-s to 442-s.

23. Savage, W. F., and Lundin, C. D. 1966. Application of the Varestraint technique to the study of weldability. *Welding Journal* 45(11): 497-s to 503-s.

24. Huang, C., and Kou, S. 2003. Liquation cracking in partial-penetration aluminum welds: Effect of penetration oscillation and backfilling. *Welding Journal* 82(7): 184-s to 194-s.

25. Cross, C. E., Gutscher, D. 2003. Effect of Cu and Fe on weldability of aluminum 2519. *6th International Trends in Welding Research Conference Proceedings*, Eds. S. A. David, T. DebRoy, J. C. Lippold, H. B. Smartt, and J. M. Vitek, Materials Park, Ohio: ASM International, pp. 638–641.

26. The Aluminum Association. 1982. *Aluminum Standards and Data.* p. 15. Washington, D.C.: The Aluminum Association.

27. Nelson, T. W., Lippold, J. C., Lin, W., and Baeslack III, W. A. 1997. Evaluation of the circular patch test for assessing weld solidification cracking, I. Development of a test method. *Welding Journal* 76(3): 110-s to 119-s.

28. Houldcroft, R. T. 1954. Dilution and uniformity in aluminum alloy weld beads. *British Welding Journal* 1: 468–472.

29. Flemings, M. C. 1974. *Solidification Processing.* pp. 34–36, pp. 160–162, and Appendix B. New York: McGraw-Hill.

30. American Society for Metals. 1986. *Binary Alloy Phase Diagrams.* Vol. 1, p. 106. Metals Park, Ohio: ASM International.

31. Singer, A. R. E., and Cotrell, S. A. 1946. Properties of the Al-Si alloys at temperatures in the region of the solidus. *Journal of Institute of Metals* 73:33–54.

32. Kou, S. 2003. *Welding Metallurgy*, 2nd edition, New York, N.Y.: John Wiley and Sons, p.151.

33. Michaud E. J., Kerr, H. W., and Weckman, D.C. 1995. *Trends in Welding Research.* Eds. H. B. Smartt, J. A. Johnson, and S. A. David, Materials Park, Ohio: ASM International, p. 154.